Flux Pinning Property in Melt-Processed Sm-123 Superconductor

T. Matsushita [a], E. S. Otabe [a],

[a] *Faculty of Computer Science and Systems Engineering, Kyushu Institute of Technology, 680–4 Kawazu, Iizuka 820–8502, Japan*

Abstract

The flux pinning property in a melt-processed Sm-123 bulk superconductor was investigated and the observed irreversibility field was compared with the theoretical model of flux creep and flow assuming that the usual condensation energy interaction by 211 particles is dominant in flux pinning. The good agreement suggests that this hypothesis is valid. The pinning mechanism around the peak effect is discussed based on the results on scaling of the pinning force density.

Keywords:

Sm-123 superconductor, Melt-process, Scaling of pinning force, Peak effect

1 Introduction

Sm-123 superconductor has a higher critical temperature than Y-123 superconductor and its anisotropy is as low as Y-123. Hence, this is a promising material for high-field applications. A pronounced peak effect is frequently observed in this material in a magnetic field applied parallel to the *c*-axis. A similar peak effect was also observed in Nd-123 superconductor and this peak effect was attributed to substituted regions of Ba by Nd with lower T_c than the surrounding matrix region with the field-induced pinning mechanism [1]. In Nd-123 system the effect of

coexistence of such substituted regions and nonsuperconducting particles of 422 phase has been investigated in detail [2,3]. It was clarified that the addition of 422 reduced the peak effect at a medium field, while the critical current density was enhanced in the low and high magnetic field regions. Although the change in the low and high fields is reasonable, the reduction in the critical current density in the medium field region seems to be peculiar. Hence, the role of these pinning centers in the observed pinning property is not clear.

In this paper the pinning property of Sm-123 bulk superconductor is investigated by measuring the irreversibility field and the scaling behavior of the pinning force density. A discussion will be given on the flux pinning mechanism in this material.

2 Experimental

The specimen was prepared by a common melt process. The nominal composition of 123 and 211 phases was selected to be 3:1 and silver was also added by 20wt%. After partial melting, the temperature was reduced and the specimen was heat-treated at 350°C for 10 h in an oxygen atmosphere. Then, the temperature was gradually reduced to 300°C in 50 h and annealed again at 300°C for 50 h. Finally the specimen was cooled down to room temperature in 12 h. The obtained melt material was cut and the size of the specimen was 1.09 mm × 2.01 mm × 2.56 mm. The *c*-axis was directed along the long axis of the specimen. The critical temperature was 94.0 K.

The critical current density was estimated from a magnetization hysteresis in a magnetic field along the *c*-axis measured using a SQUID magnetometer. The irreversibility field was conventionally determined by the magnetic field at which the critical current density is reduced to 1.0×10^6 A/m^2.

Fig. 1 shows the critical current density at various magnetic

fields and temperatures. It is seen that the peak effect is observed in a wide temperature region from 40 to 85 K. A shoulder can be seen up to much higher temperature. The irreversibility field, $B_{\rm i}$, is represented in Fig. 2. The obtained irreversibility line is smooth in the range of our measurement. Since a trace of the peak effect seems to remain even above 85 K as seen in a shoulder, the "peak" field was defined by the field at which the second derivative of $J_{\rm c}$-B curve takes a negative maximum. The result is shown in Fig. 2. It is about 40 % of the irreversibility field.

Fig. 3 shows the scaling of the pinning force density, where $B_{\rm i}^*$ is the effective irreversibility field at which the extrapolated $J_{\rm c}$ reaches zero. When the magnetic field is normalized by the usual irreversibility field, $B_{\rm i}$, the scaling at high fields is not beautiful. $B_{\rm i}^*$ is slightly higher than $B_{\rm i}$. The scaled pinning force density has a long tail at high fields, take maximum at around the normalized field of 0.4 and is widely spread at normalized field below 0.4. Such an obtained deterioration at lower fields is different from a behavior in Nd-123 system [3]. The reason for this deterioration will be discussed later. The temperature dependence of the maximum pinning force density is shown in Fig. 4. It obeys approximately as

$$F_{\rm pmax} \propto \left[1 - \left(\frac{T}{T_{\rm c}}\right)^2\right]^{3.0} . \qquad (1)$$

3 Discussion

The present specimen is expected to contain sufficient volume fraction of 211 phase particles. Hence, the pinning property at low fields is considered to obey the formula for the normal precipitate pinning [4]. In fact, the obtained pinning parameters describing the temperature and magnetic field dependencies are close to the prediction [5]. In Nd-123 system, addition of 422 particles contributed to the larger pinning at high fields [3],

suggesting that the 422 phase particles again dominate the pinning property. The strange behavior at medium fields by addition of 422 phase is explained as follows [6]: The substituted regions with lower T_c is speculated to work as strong repulsive pinning centers under the proximity effect because of the large kinetic energy resulted from the longer coherence length. In the low field region the spacing of flux lines is fairly long, resulting in no strong interference between positive(kinetic) and negative(condensation) energies for pinning. Hence, the pinning force is considered to simply increase with increasing 422 particles. In the medium field region, the interference becomes stronger through the elasticity between flux lines and the critical current density is speculated to decrease by the offset of the two kinds of pinning energies. At higher fields, it is considered that the superconductivity in the substituted regions diminishes to avoid the state of very high kinetic energy due to the existence of flux lines inside the substituted region, since flux lines always exist during their displacement along the direction of the Lorentz force. In this case the superconductivity in surrounding matrix is also degraded due to the proximity effect. Hence, only the attractive condensation interactions by 422 particles remain. Thus, this scenario explains all the behavior observed in [3]. This indicates that the irreversibility field is mainly explained by the pinning by 211 phase in the present Sm-123 bulk specimen, although the pinning property is considered to be slightly degraded due to the proximity effect.

The irreversibility field is theoretically estimated using the flux creep-flow model [7]. In the theoretical model, the most important quantity is the pinning potential and this can be theoretically estimated by the virtual critical current density in the creep-free case, J_{c0}, which is used as a parameter representing the pinning strength. In the present case, J_{c0} can be analytically derived as [4]:

$$J_{c0} = \frac{\pi B_c^2 \xi_{\parallel} N_p D^2}{4\mu_0 B a_f} \left(1 - \frac{B}{B_{c2}}\right)^{\delta}, \tag{2}$$

where B_c is the thermodynamic critical field, $\xi_{\|}$ is the coherence length in the a-b plane, N_p is the number density of 211 particles, D is the particle size and a_f is the flux line spacing. Thus, if we express this as

$$J_{c0} = A\left[1 - \left(\frac{T}{T_c}\right)^2\right]^m B^{\gamma-1}\left(1 - \frac{B}{B_{c2}}\right)^\delta, \tag{3}$$

we have $m = 3/2$, $\gamma = 1/2$. The parameter representing the magnitude of J_{c0}, A, was assumed to be distributed as

$$f(A) = K \exp\left[-\frac{(\log A - \log A_m)^2}{2\sigma^2}\right], \tag{4}$$

where A_m is the most probable value of A, σ is a parameter representing the degree of deviation and K is a constant. Here we assume that A_m and σ^2 are adjusting parameters to get a good agreement between the theory and experiment for the irreversibility field. The assumed parameters are: $A_m = 6.0 \times 10^7$, $\sigma^2 = 0.1$, $\delta = 2$. Using these values, the mean number of flux lines in the flux bundle is estimated as 4.3. E-J characteristics were calculated and the critical current density was determined at the electric field criterion of $E = 10^{-11}$ V/m so as to be consistent with the DC magnetization measurement. The irreversibility field was determined using the same criterion as experiment. The obtained result is shown in Fig. 2 for comparison. The agreement is satisfactory.

This agreement seems to support the above hypothesis that 211 particles are again dominant in the flux pinning at high fields. This is also consistent with the agreement in E-J characteristics in these fields, which are estimated from the relaxation of magnetization [5]. The number of A_m assumed here may seem to be too small. However, since the superconductivity in the matrix around the substituted regions is speculated to be deteriorated due to the proximity effect, the reduction in A_m seems to be natural.

Here we shall discuss the scaling behavior of the pinning force

density. The long tail at high fields is pronounced in the scaled curve. This comes from the sharp drop in J_c above the peak field. The sharp drop is considered to originate from the disappearance of the kinetic energy interaction due to the disappearance of the superconductivity in the substituted region, as argued above. Another characteristic point of the observed scaling behavior is that the pinning force in the magnetic field region below the peak is not exactly scaled. This may be partly ascribed to the different pinning mechanisms between the medium and high field regions. That is, the peak effect is considered to be mainly brought about by the kinetic energy interaction by the substituted regions, while the pinning near the irreversibility field is speculated to be caused by the usual condensation energy interaction by 211 particles. In addition, the appreciable reduction in the peak effect at high temperatures is also one of the reasons for such a deviation from a perfect scaling.

4 Summary

The flux pinning property in a melt-processed Sm-123 bulk specimen with 211 particles was investigated and the following results were obtained.

(1) The irreversibility field was qualitatively explained by assuming the pinning interactions by 211 particles. This supports the hypothesis that these particles are dominant at high fields.
(2) The observed deviation from the perfect scaling of the pinning force density near the peak seems to be consistent with the assumption that the pinning mechanism is different between the substituted regions and the 211 particles.

5 Acknowledgments

The authors would like to acknowledge Drs. M. Morita and T. Tokunaga of Nippon Steel Corporation for preparing the melt processed Sm-123 specimens for the measurement.

References

[1] N. Chikumoto and M. Murakami, Proc. 10th Anniv. HTS Workshop, 1996, p. 138.

[2] H.Kojo, S. I. Yoo, N. Sakai and M. Murakami, Adv. Supercond. IX (Springer, Tokyo, 1997) p. 717.

[3] T. Mochida, N. Chikumoto, T. Higuchi and M. Murakami, Adv. Supercond. X (Springer, Tokyo, 1998) p. 489.

[4] T. Matsushita, E. S. Otabe, B. Ni, K. Kimura, M. Morita, M. Tanaka, M. Kimura, K. Miyamoto and K. Sawano, Jpn. J. Appl. Phys. **30** (1991) L342.

[5] E. S. Otabe and T. Matsushita, to be published in Adv. Supercond. XII (Springer, Tokyo, 2000).

[6] T. Matsushita, 2nd Int. Works. on Processing and Applications of Superconducting (RE)BCO Large Grain Materials, Morioka, October 1999.

[7] M. Kiuchi, K. Noguchi, T. Matsushita, T. Kato, T. Hikata and K. Sato, Physica C **278** (1997) 62.

Figure captions

Fig. 1. Critical current density of Sm-123 bulk specimen under a magnetic field along the *c*-axis.

Fig. 2. Irreversibility field vs temperature. Solid and broken lines represent the observed and calculated results, respectively. Open symbols are the peak fields.

Fig. 3. Scaling of the pinning force density.

Fig. 4. Temperature dependence of the maximum pinning force density.

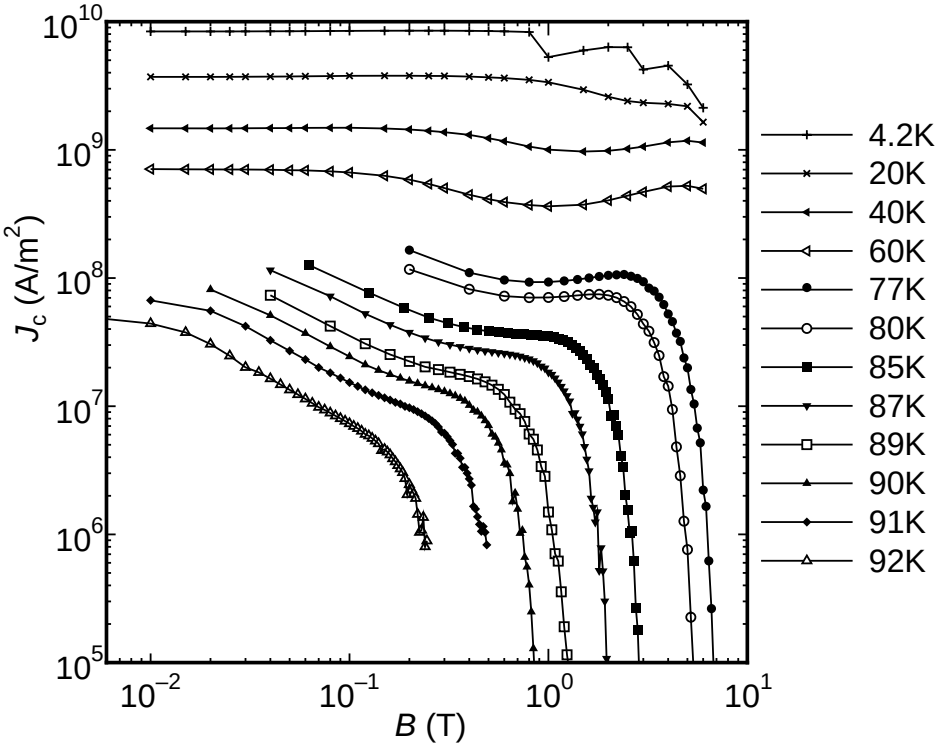

Figure 1. T. Matsushita and E. S. Otabe

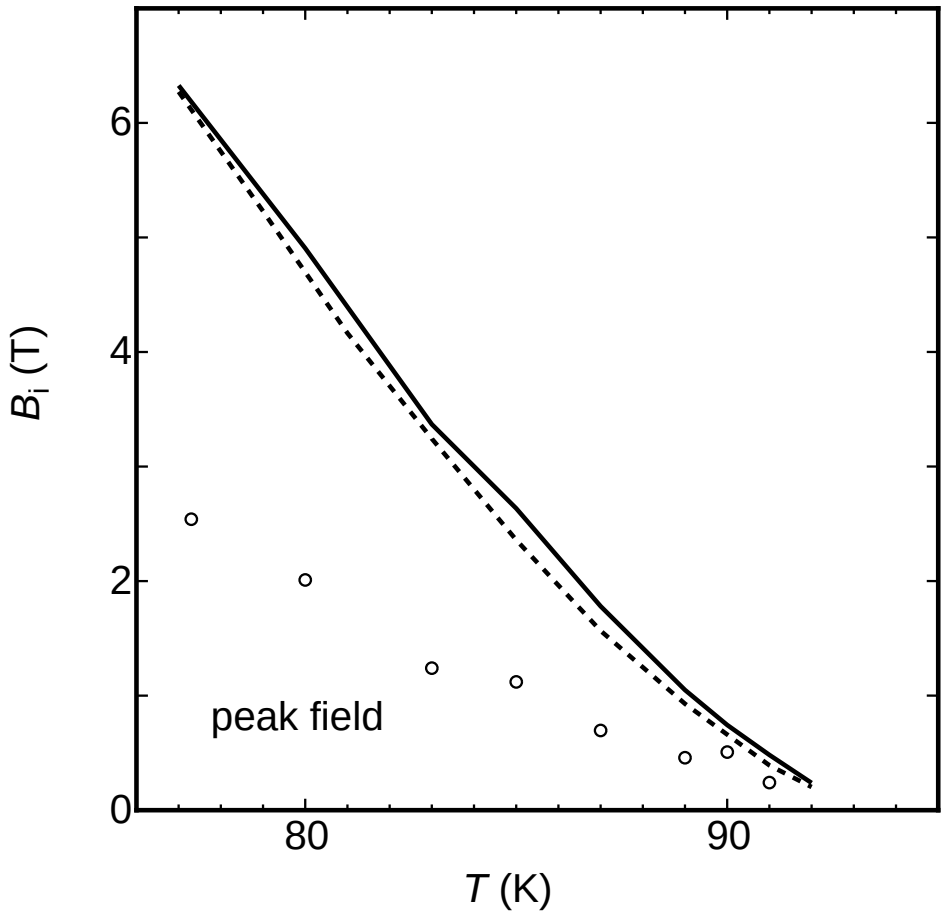

Figure 2. T. Matsushita and E. S. Otabe

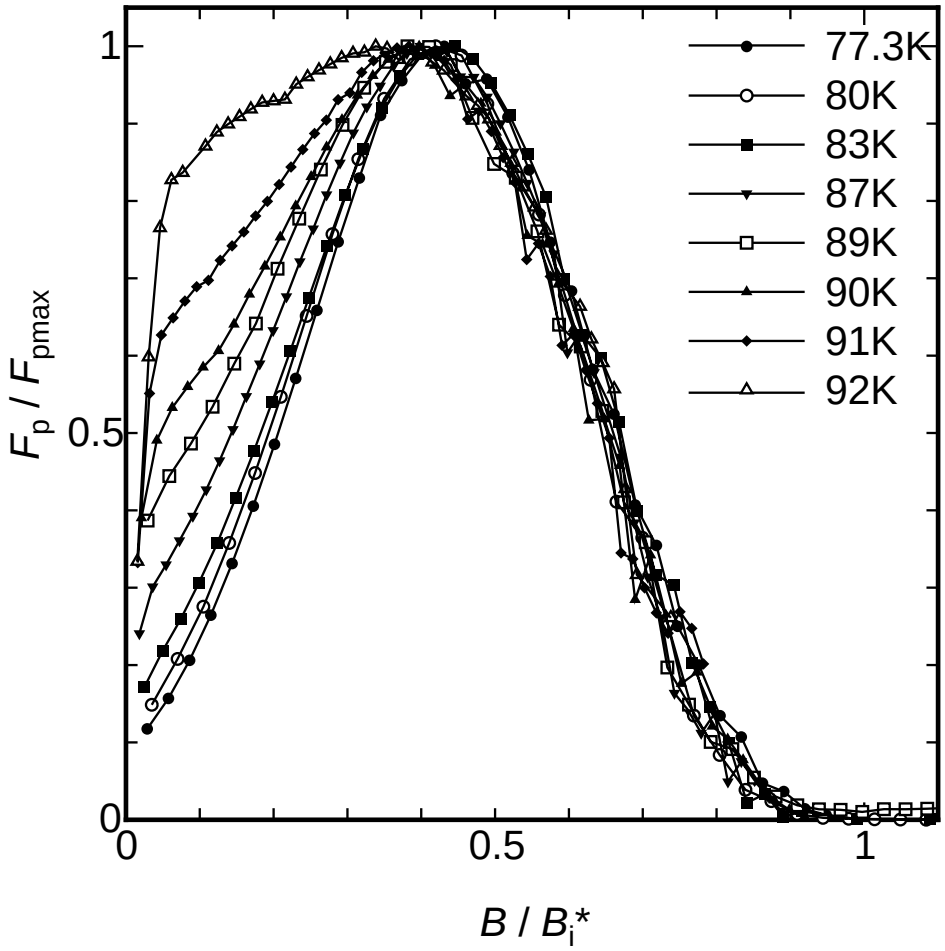

Figure 3. T. Matsushita and E. S. Otabe

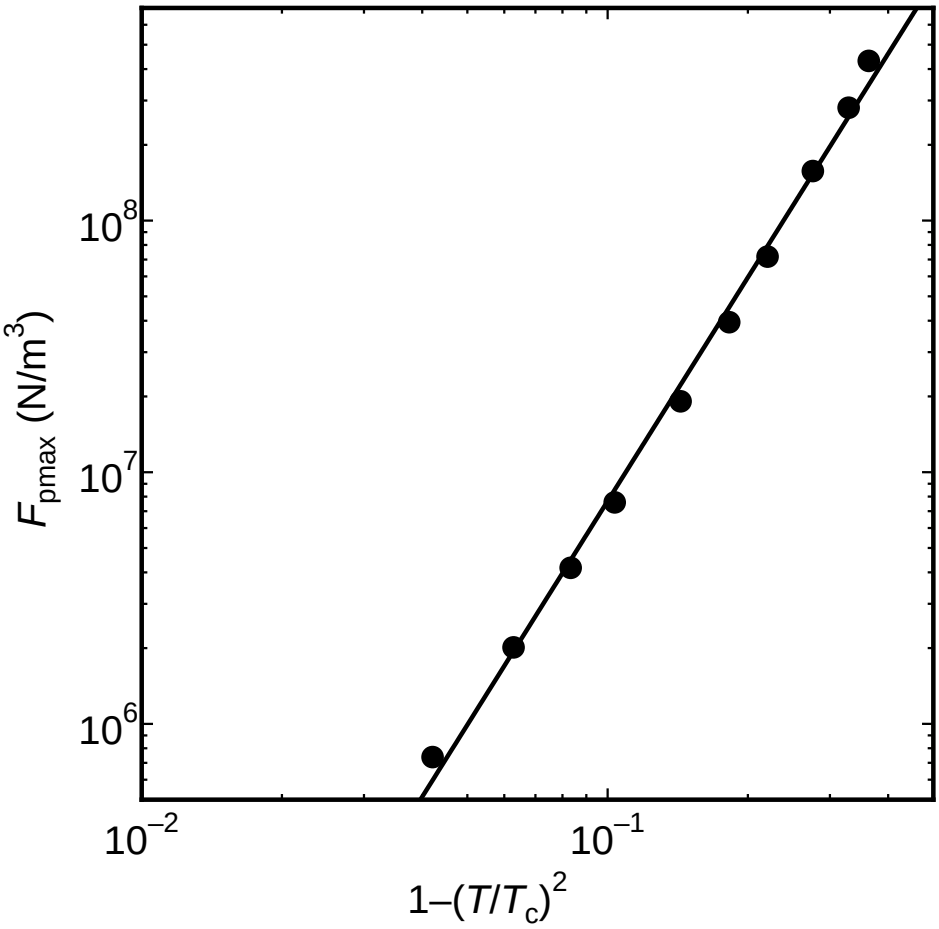

Figure 4. T. Matsushita and E. S. Otabe